Available online at www.sciencedirect.com

ScienceDirect

Procedia Engineering 86 (2014) 42 – 50

Procedia Engineering

www.elsevier.com/locate/procedia

1st International Conference on Structural Integrity, ICONS-2014

Assessment of Mechanical Property of Ti-5Ta-2Nb and 304L SS Explosive Clad and Correlation with Microstructure

C. Sudha*, T.N. Prasanthi, V. Thomas Paul, S. Saroja and M. Vijayalakshmi

Physical Metallurgy Group, Metallurgy and Materials Group
Indira Gandhi Centre for Atomic Research, Kalpakkam - 603102, India
**E-mail ID: sudha@igcar.gov.in*

Abstract

Spent fuel reprocessing plants of FBRs require advanced structural materials for service in aggressive conditions. Ti-5Ta-2Nb is a candidate structural material for electrolytic dissolver whereas 304L SS is used for rest of the plant. 'Zero failure' requirement for the process vessels necessitated the development of defect free explosive clad between Ti-5Ta-2Nb and 304L SS. The paper deals with the investigations carried out on the mechanical properties and microstructure of the explosive clads, and modification in microstructure on subsequent thermal exposure. The structural integrity of the clad as a consequence of these structure-property changes is also discussed in the paper.

Peer-review under responsibility of the Indira Gandhi Centre for Atomic Research

Keywords: Ti-5Ta-2Nb, 304L SS, Explosive cladding, bond strength, diffusion zones

1. Introduction

Spent fuel from fast breeder reactors that contain high concentration of plutonium, fission products and transuranium elements is reprocessed by a special electro-oxidative dissolution process [1]. Nitric acid at various levels of concentration and temperature is used as the main process medium in different parts of the reprocessing circuit. An α-β Ti alloy, Ti-5Ta-2Nb (TiTaNb) with superior corrosion resistance than grade-1 Ti is a possible structural material for service in concentrated HNO_3 containing highly oxidizing ions [2]. In such a case, the dissolver made of TiTaNb has to be joined to rest of the process vessels and piping fabricated using 304L austenitic stainless steel (304L SS).

Peer-review under responsibility of the Indira Gandhi Centre for Atomic Research
doi:10.1016/j.proeng.2014.11.009

Achieving good quality joint between TiTaNb and 304L SS is a challenge due to a number of factors such as (a) limited mutual solubility of Fe and Ti (b) strong tendency for the formation of intermetallic phases and (c) difference in thermal expansion coefficient. Detailed investigations carried out on Ti/304L SS dissimilar joints showed explosive cladding to be a promising method of joining [3].

Explosive cladding is a cold pressure welding process where detonation of an explosive accelerates the cladding plate (TiTaNb, in the present study) to a very high velocity which then collides with the base plate to form metallurgical bond by severe plastic deformation [4]. It was successfully demonstrated for joining both similar and dissimilar materials like Cu-Cu, Al-Al, Cu-Ti, Cu-SS, Al-Mg and Ti-SS [5-10]. Compared to conventional fusion welding techniques an explosive cladding process is advantageous because it eliminates (1) melting of the base materials (2) interdiffusion/dilution of alloying elements and (3) formation of a continuous network of deleterious phases parallel to the clad interface. Hence, explosive cladding technique was used to join TiTaNb to 304L SS. The highly corrosive and radioactive operating conditions in the plant and the difficulties associated with maintenance, demand sound and high quality joints. Hence, qualification of this dissimilar clad with respect to defects, design properties and stability is crucial.

This paper presents the results on assessment of the bond strength of Ti-5Ta-2Nb and 304L SS explosive clads and correlation of the observed changes in property with microstructure. Thermal stability of the explosive clad is investigated with respect to the propensity for formation of intermetallic phases and a safe temperature-time limit is proposed for any post processing operations.

2. Experimental Methods

2.1 Fabrication of Explosive Clads

Table 1 and 2 show the chemical composition and mechanical property of the starting materials. TiTaNb plate of dimension 250x450x6mm was clad on 304L SS plate of dimension 250x400x6mm by explosive cladding process, details of which are given elsewhere [11]. TiTaNb with lower tensile (UTS) and yield strength (YS) was used as the flier plate and 304L SS as the base plate. Ultrasonic examination revealed de-bonding at the clad edges (Fig. 1) which was removed prior to extracting specimens for further studies. The clads were also heat treated in the temperature range of 823-1073K for 1 to 20h.

Table 1 Chemical composition (in wt%) of the plates used in the study

Element	C	Si	Mn	S	P	Cr	Ni	N	Fe	H	O	Ta	Nb	Ti
304L SS	0.02	0.57	1.66	0.004	0.03	18.15	8.59	0.03	Bal	-	-	-	-	-
TiTaNb	0.01	0.03	-	-	-	0.1	0.1	0.01	0.2	0.04	0.42	4.2	1.9	Bal

Table 2 Mechanical properties of plates used in the study

304L SS	
YS (MPa) (average)	280
UTS (N/mm^2) (average)	566
% Elongation (average)	62
TiTaNb	
0.2% proof strength (MPa)	256-266 (longitudinal)
UTS (MPa)	418-412 (longitudinal)
% elongation	37-40 (longitudinal)

2.2 Mechanical Property Evaluation

Variation of hardness across the clad interface was determined using Leitz microhardness tester with an applied load of 100g. Bond strength of the clad was assessed by longitudinal and transverse tensile and bend tests in addition to shear test. For testing in longitudinal direction, restriction with respect to clad thickness necessitated the fabrication of subsized specimens as per ASTM E8 and E90 for tensile (Fig. 2(a)) and bend test (Fig. 2(b)) respectively. Room temperature tensile testing was carried out on 304L SS, TiTaNb and explosive clad (with tensile axis parallel to the interface) whereas bend test was carried out only on the clad. Shear test specimens had dimension as per ASTM A264 (Fig. 3). For tensile and bend test in transverse direction (tensile axis perpendicular to clad interface) as per ASTM 308 it was necessary to fabricate similar welds of TiTaNb and 304L SS as shown in Fig. 4(a) and (b).

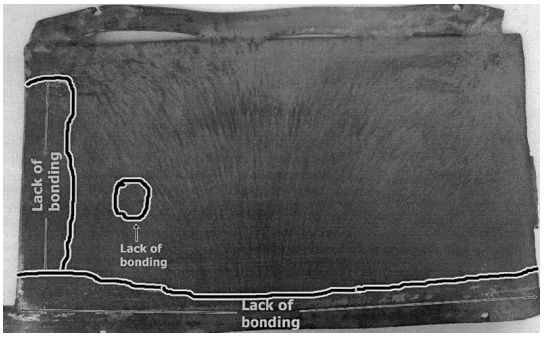

Fig. 1 Result of ultrasonic testing showing de-bonding at the clad edges

2.3 Microstructural and Microchemical Characterization

Cross-section of the clad was prepared by standard metallography procedures and etched using Kroll's reagent and HCl+ HNO_3+distilled water on TiTaNb and SS side respectively.

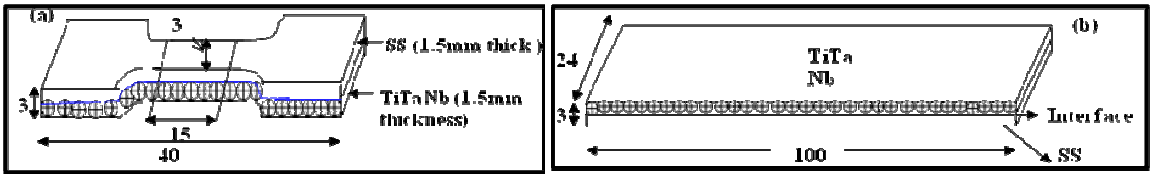

Fig. 2 Schematic of specimens used for (a) tensile and (b) bend tests in longitudinal direction (dimensions in mm)

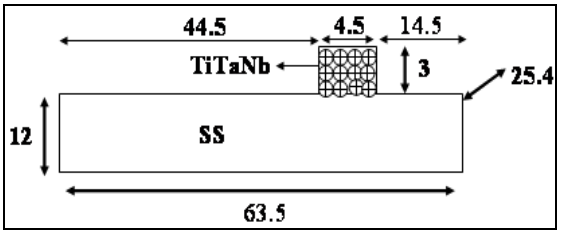

Fig. 3 Schematic of specimen used for shear test (dimensions in mm)

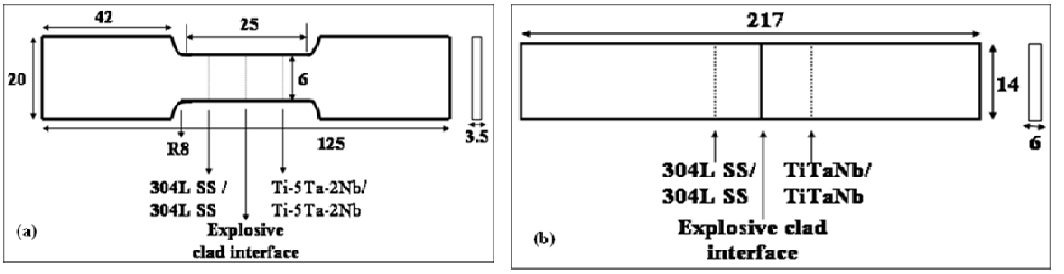

Fig. 4 Schematic of specimens used for (a) tensile and (b) bend tests in transverse direction (dimensions in mm)

Scanning electron microscope (FEI XL30 SEM) equipped with EDS was used for microstructural observation. Microchemical characterization was performed with electron microprobe (Cameca SX50 EPMA) at an accelerating voltage and current of 20kV and 20nA respectively. Characteristic X-ray intensities were corrected for

atomic number, absorption and fluorescence effects for quantification. Philips CM200 transmission electron microscope (TEM) was used to study thin foil specimens at 200kV.

3. Results and Discussion

3.1 Mechanical Property Evaluation of Base and Flier Plates

Stress-strain curves and fractographs obtained for 304L SS and TiTaNb post cladding are given as Fig. 5(a) and (b) respectively. UTS, YS and % elongation for 304L SS and TiTaNb are (640MPa, 530MPa, 53) and (460MPa, 80MPa, 20) respectively. Both SS and TiTaNb showed ductile mode of failure (insets in Fig. 5(a) and (b)) but 304L SS had higher ductility than TiTaNb and had higher UTS and YS than the starting material (Table 2). TiTaNb exhibited extremely low YS (80MPa) after explosive cladding which can be understood as follows: TiTaNb had an α-β structure prior to explosive cladding. Severe deformation undergone by the material during cladding resulted in the formation of a metastable fcc phase of Ti (volume fraction - ~0.63) in addition to parent α and β phases [12]. In an earlier investigation [13] on variation in Gibb's free energy with temperature and crystallite size in commercially pure Ti, it was concluded that fcc phase was preferred for small (nm range) crystallite sizes. The skewed stress-strain curve (Fig. 5(b)) suggested highly localized deformation possibly resulting in the formation of micron and nano metre sized crystallites thereby stabilizing the fcc phase. Since the effect of fcc phase on mechanical property of Ti is unknown it can only be speculated that very low YS is probably a result of (a) highly localized deformation of the material and (b) deformation induced phase transformation.

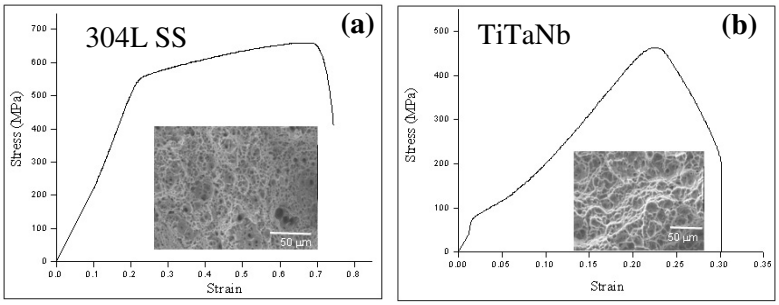

Fig. 5 Stress-strain curves and fractographs (as inset) obtained after explosive cladding

3.2 Microstructural Changes in 304L SS Base Plate

To understand the observed changes in mechanical property of 304L SS base plate, microstructure and hardness post the cladding operation were examined. 304L SS had deformed microstructure (Fig. 6) with high hardness (~375VHN) suggesting that it has undergone severe plastic deformation during explosive cladding. Detailed electron microscopy investigations [12] confirmed the formation of both bcc (α') and hcp (ε) martensite supporting the high YS, UTS and reduction in ductility obtained for the base plate.

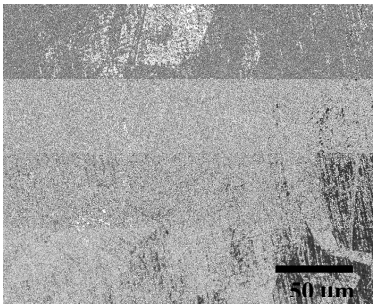

Fig. 6 Microstructure of 304L SS after explosive cladding

3.3 Mechanical Property Evaluation of the Explosive Clad

Figure 7(a) shows the hardness profile obtained across the cross section of the clad. Near the interface on the SS side hardness was high (~425VHN) indicating reduction in ductility of the clad. Stress-strain curves along longitudinal and transverse directions are given as Fig. 7(b) and (c) respectively. In longitudinal direction average values for UTS, YS and % elongation were obtained as 740MPa, 200MPa and 6 respectively. De-bonding observed at the interface (inset as Fig. 7(b)) explained the observed reduction in ductility. In transverse direction, UTS (301MPa) and YS (276MPa) had lower values compared to base material (Table 2). Bend test yielded included angle as 110 and < 5˚ along longitudinal and transverse directions. Closer examination of these specimens also revealed tearing along joint interface.

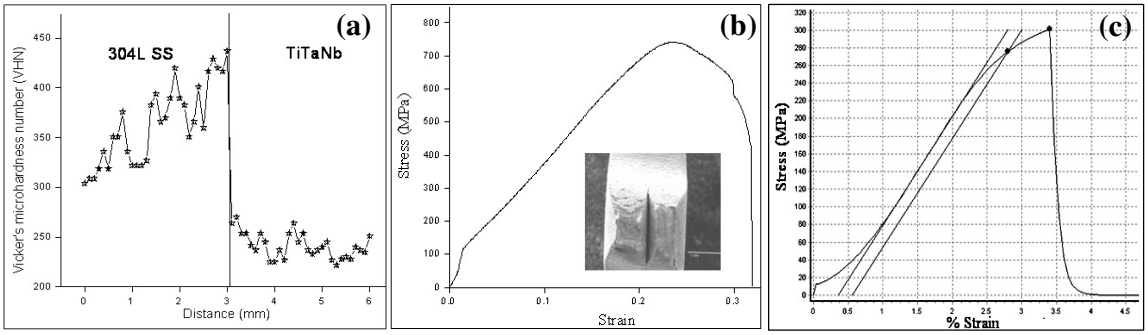

Fig. 7 (a) Hardness profile; Stress vs strain curves and fractographs (as inset in (b)) for the clad along (b) longitudinal and (c) transverse directions

Figure 8(a) shows the overall view of the test piece before and after shear testing. Shear strength values varied between 293-450MPa similar to that obtained for Ti/304 SS explosive clads [14]. Fracture surface (Fig. 8(b)) showed combined brittle and ductile mode of failure. EDS spectra (inset in (b)) showed equal intensities for Fe and Ti in few regions suggesting the presence of brittle intermetallic phases in isolated pockets at the clad interface.

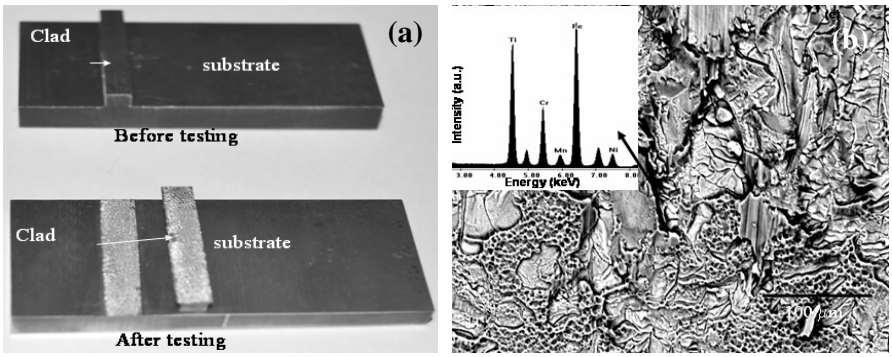

Fig. 8 (a) Specimen used for shear testing (b) fracture surface showing combined ductile-brittle mode of failure; inset is the EDS spectrum obtained from arrow marked region

3.4 Interface Microstructure of the Explosive Clad

Figure 9(a) shows the microstructure of the cross section of 'as received' explosive clad. The clad interface was found to be sharp and wavy with occasional presence of vortices. Elemental concentration profiles obtained using EPMA (Fig. 9(b)) showed no evidence for inter-diffusion of alloying elements within its resolution limit suggesting the absence of intermetallic phases at the interface.

Electron microscopy investigations were carried out on cross section specimens extracted from the explosive clad. TEM bright field images, EDS spectra and electron diffraction patterns obtained as a function of distance from the clad interface are shown in Fig. 10. 304L

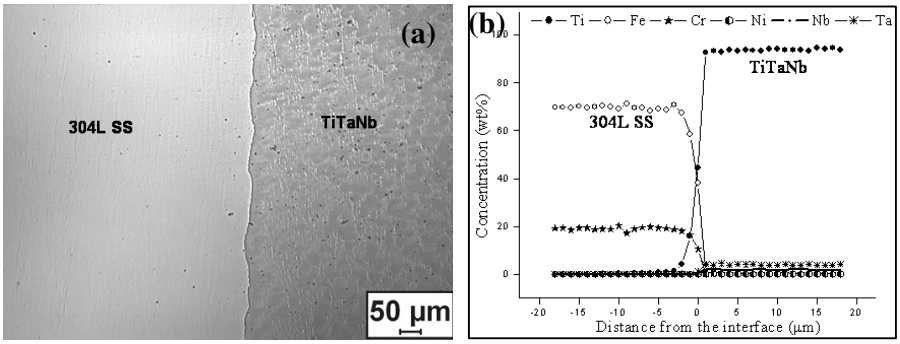

Fig. 9 (a) Microstructure obtained from the cross section of the clad (b) Elemental concentration profiles obtained using EPMA

SS base plate showed the presence of shear bands (Fig. 10(a)) and confirmatory evidence was obtained for the presence of α-Fe (bcc) phase at their intersections (Fig. 10(c)). Near the interface on SS side there was high number density of dislocations present along with shear bands (Fig. 10(d)). Approximate composition in this region was 71Fe-10Cr-17Ni-2Ti (Fig. 10(e)). Right at the interface (Fig. 10(f)) where the composition was obtained as 36Fe-9Cr-55Ti (Fig. 10(g)) evidence existed for the presence of FeTi intermetallic phase (Fig. 10(h)). Further, near the interface in TiTaNb, α(hcp) grains were elongated (Fig. 10(i)) and approximately 20wt% of Fe was present. Even though the concentration of Fe, a β stabilizer was quite high in this region no experimental evidence existed for the presence of β phase. EPMA profiles (Fig. 9(b)) also did not indicate interdiffusion of alloying elements. Hence higher concentration of Fe obtained through EDS analysis may be due to the acquisition of X-ray intensities from both SS and TiTaNb sides. Well away from the clad interface the microstructure and chemistry was similar to that of the flier plate (Fig. 10(k) to (m)). TEM investigations further strengthened the suggestion that in 'as received' explosive clads intermetallic phases are present at isolated pockets at the interface.

Detailed analysis of explosive clad thus confirmed that it is unsuitable for service in 'as clad' condition. Formation of deformation induced martensite in SS will drastically affect the mechanical property of the clad. Unlike in fusion welded joints though intermetallic phases are not present as distinct zones parallel to the interface, transverse tensile and bend tests did not yield satisfactory result. Evidence existed for the presence of intermetallic phases preferably in vortex regions as inferred from shear testing (Fig. 8(b)) and TEM analysis (Fig. 10). Though explosive cladding is a non-fusion welding process localized melting of metals is possible due to: (1) adiabatic heating of gases compressed between plates (2) internal heating of component metals due to passage of shock waves and (3) heat of detonation of the explosive [4]. In these regions there is high probability for the formation of intermetallic phases. Heat treatment of explosive clad is reported [14] to be beneficial for removing the stresses and improving the bond strength. However, prolonged exposure at high temperature may be detrimental. Hence, evolution of interface microstructure with heat treatment was studied and formation of various phases at clad interface was predicted as described below:

3.5 Formation of Reaction Zones at the Clad Interface after Thermal Exposure

Explosive clads were heat treated in the temperature range of 823 to 1073K for 1 to 20h. For lower temperature of heat treatment (823K) the interface was wavy, sharp and easily distinguishable with no microstructural change indicating the formation of reaction zones. At 873K a dark zone with a concomitant increase in hardness (350VHN) (Fig. 11(a)) appeared at the interface after 10h of exposure. This dark zone appeared as a continuous band with an average width of 4µm. Number and width of the diffusion zones increased with heat treatment temperature and time due to enhanced interdiffusion of alloying elements (Fig. 11(b)). At 1073K total diffusing distance for Fe in TiTaNb side was ~45 and 330µm after 1 and 20h. Concentration profiles obtained using EPMA (Fig. 11(c)) indicated the formation of Fe and Ti rich intermetallic phases in the dark zone which was later confirmed through cross section electron microscopy. Enhancement in Cr (30-40at%) on SS side was attributed to the formation of σ phase. With the diffusion of Fe, a β(bcc) phase stabilizer into TiTaNb, the high temperature bcc phase was stabilized to form a wide zone (labeled 'B') adjacent to dark region (labelled 'A') (Fig. 11(b)). As the concentration of Fe reduced the β phases became unstable resulting in the formation of Widmanstatten α-β structure (labelled 'C' in Fig. 11(b)). Probability for the formation of various phases was predicted using JMatPro, a material

modeling software. Figure 11(d) is the predicted change in the mole fraction of α(hcp), β(bcc) and FeTi phases in TiTaNb with change in the concentration of Fe.

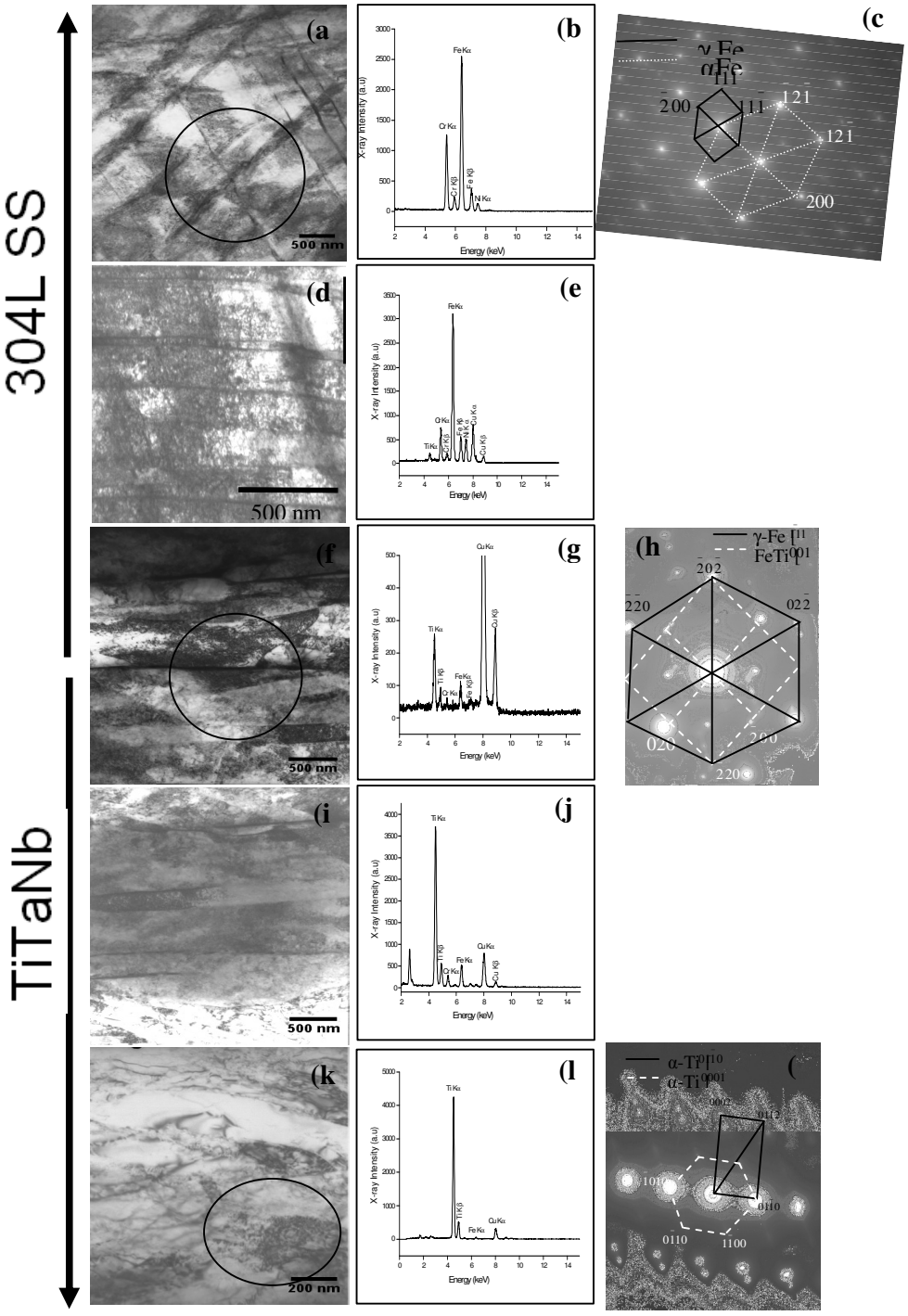

Fig. 10 TEM bright field image, EDS spectra and SAD patterns obtained as a function of distance from the clad interface

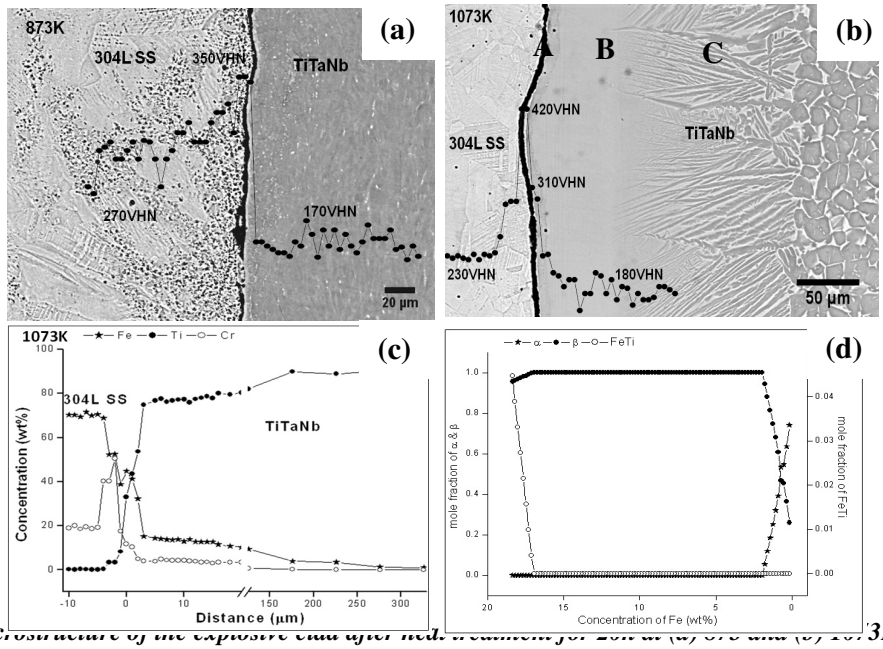

Fig. 11 Microstructure of the explosive clad after heat treatment for 20h at (a) 873K and (b) 1073K; (c) Concentration profiles across the clad after heat treatment at 1073K for 20h (d) Predicted mole fraction of various phases vs concentration of Fe in TiTaNb

4. Conclusion

- Explosive cladding of Ti-5Ta-2Nb on 304L SS resulted in deformation induced phase transformation in stainless steel.
- Formation of deformation induced martensite in 304L SS lead to increase in UTS and YS and decrease in ductility.
- Bond strength in the longitudinal direction was satisfactory whereas in the transverse direction the clad did not meet the specifications.
- Intermetallic phases were not detected in 'as received' explosive clads within the

  resolution limit of an electron microprobe. However electron microscopy investigations suggested their presence at isolated pockets at the clad interface.
- Heat treatment of the explosive clads have to be restricted to temperatures <873K and durations below 10h to avoid the formation of a continuous network of intermetallic phases parallel to the clad interface.

Acknowledgement

The authors would like to express their sincere thanks to Dr. P.R. Vasudeva Rao, Director IGCAR and Dr. T. Jayakumar, Director, Metallurgy and Materials Group, IGCAR for their encouragement and support during the course of this work. The authors would like to thank Mr. G. Kempulraj and Mr. T. Saravanan of Central workshop, IGCAR for their help in fabricating the specimens and Mr. M. Nandagopal and Miss. S. Panneerselvi, MDTG, IGCAR for their help in mechanical property evaluation.

References

1. Raj B, and Kamachi Mudali U, Prog Nucl Energy 48 (2006) 283.
2. Mythili R, Thomas Paul V, Saroja S, Vijayalakshmi M, and Raghunathan V S, Mater Sci Engg A 390 (2005) 299.
3. Kamachi Mudali U, Ananda Rao B M, Shanmugam K, Natarajan R, and Baldev Raj, J Nucl Mater 321 (2003) 40.
4. Tamhankar R V, and Ramesam J, Mater Sci Engg 13 (1974) 245.
5. Dor Ram Y, Weiss B Z, and Komem Y, Acta Metall 27 (1979) 1417.
6. Grignon F, Benson D, Vecchio K S, and Meyers M A, Int J Impact Engg 30 (2004) 1333.
7. Kacar R, and Acarer M, Mater Sci Engg A 363 (2003) 290.
8. Kahraman N, and Gulenc B, J Mater Process Technol 169 (2005) 67.
9. Raghukandan K, J Mater Process Technol 139 (2003) 573.
10. Fendik F, Mater Design 32 (2011) 1081.
11. Sudha C, Prasanthi T N, Murugesan S, Saroja S, Kuppusami P, and Vijayalakshmi M, Sci Technol Weld Join 14 (2009) 597.
12. Sudha C, Prasanthi T N, Thomas Paul V, Saroja S, and Vijayalakshmi M, Metall Mater Trans A 43 (2012) 3596.
13. Xiong S, Qi W, Huang B, Wang M and Li Y, Mater Chem Phy 120 (2010) 446.
14. Crossland B, and Williams J D, Metall Reviews 144 (1970) 79.
15. Ghosh M, and Chatterjee S, Mater Sci Engg A 35